Vietnam Journal of Mechanics, NCST of Vietnam Vol. 21, 1999, No 1 (57 - 64)

STUDY OF PRESTRAIN INFLUENCE FOR THE PREDICTION OF THE NECKING OCCURRENCE

NGUYEN NHAT THANG
Hanoi University of Technology

ABSTRACT. This paper contains experimental results for mechanical characteristics of a mild steel sheet. The determination of the forming limit stress curve for solicitation along two direction is drawn. Study of prestrain influence from the limit stress diagram is presented.

§1. Introduction

The industrial blank usually show complex strain-paths, so the use of forming limits diagram, draw for rectilinear strain-paths can not allow to predict the success of a drawing operation in press shop.

In some works we have seen the existence of a single forming limits stress curve which is independent on the strain path shape, while the classical forming limit curves are dependent on them for an orthotropic sheet-steel [2], [3], [6]. In previous work [11], we have shown the strain path influence on the forming limit diagram. Here, we determine the stress states at the onset of necking for rolling and transverse directions of sheet-steel. Then we present the forming limit diagrams calculated for different prestrains.

§2. Determination of the forming limits stress curves for solicitation along rolling and transverse directions

The experimental results have been obtained from a mild steel sheet named SE DDR-T700 of thickness 0.68 mm.

- Elastic limits along the rolling and transverse directions

$$\sigma_0 = 166; \qquad \sigma_{90} = 170 \text{ (MPa)}$$

- Landkford's coefficients along two directions:

$$r_0 = 1.5; \qquad r_{90} = 1.85$$

Variation of two coefficients is presented on Fig. 1

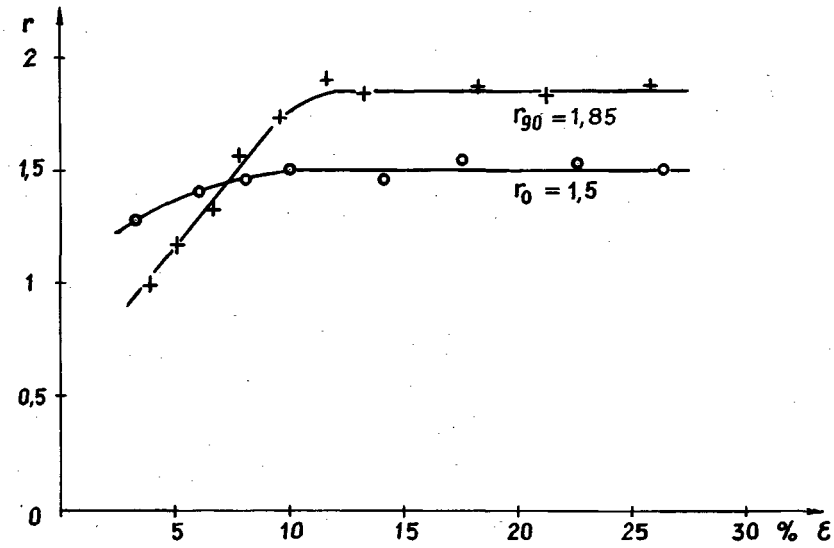

Fig. 1. **Variation of anisotropic coeficient**

- Hill's coefficients [5]

$$F = 1.1; \quad G = 1.3; \quad H = 2.3 \quad (MPa^{-1/2}).$$

The forming limit diagrams are determined by means of a Marciniak's device. The strain at the onset of necking are determined by means of a step to step strain nanalysis of a grid network laid on the samples surface [4]. They are plotted allong the rolling and transverse directions (Fig. 2)

The normality rule of the plastic flow can be written in the following way

$$d\varepsilon_{ik}^{p} = d\lambda\left(\partial f / \partial \sigma_{ik}\right). \tag{2.1}$$

According to Hill's criterion [2], the plastic strain increments can be determined with the following relations

$$\begin{aligned}
d\varepsilon_x &= d\lambda\left[G(\sigma_x - \sigma_z) + H(\sigma_x - \sigma_y)\right] \\
d\varepsilon_y &= d\lambda\left[F(\sigma_y - \sigma_z) + H(\sigma_y - \sigma_x)\right] \\
d\varepsilon_z &= d\lambda\left[G(\sigma_z - \sigma_x) + F(\sigma_z - \sigma_y)\right] \\
d\varepsilon_{xy} &= d\lambda N\sigma_{xy} \\
d\varepsilon_{zx} &= d\lambda M\sigma_{zx} \\
d\varepsilon_{yz} &= d\lambda L\sigma_{yz}
\end{aligned} \tag{2.2}$$

The effective stress $\overline{\sigma}$ is calculated by the relation (we consider transverse direction x as reference direction)

$$\overline{\sigma}^2 = \frac{1}{(G+H)}\Big[F(\sigma_y - \sigma_z)^2 + G(\sigma_z - \sigma_x)^2 + H(\sigma_x - \sigma_y)^2 + 2L\sigma_{yz}^2 + 2M\sigma_{xz}^2 + 2N\sigma_{xy}^2\Big]. \tag{2.3}$$

The coefficient $d\lambda$ can be written

$$d\lambda = \frac{d\overline{\varepsilon}}{(G+H)\overline{\sigma}} \tag{2.4}$$

where $d\overline{\sigma}$ - effective stress increment.

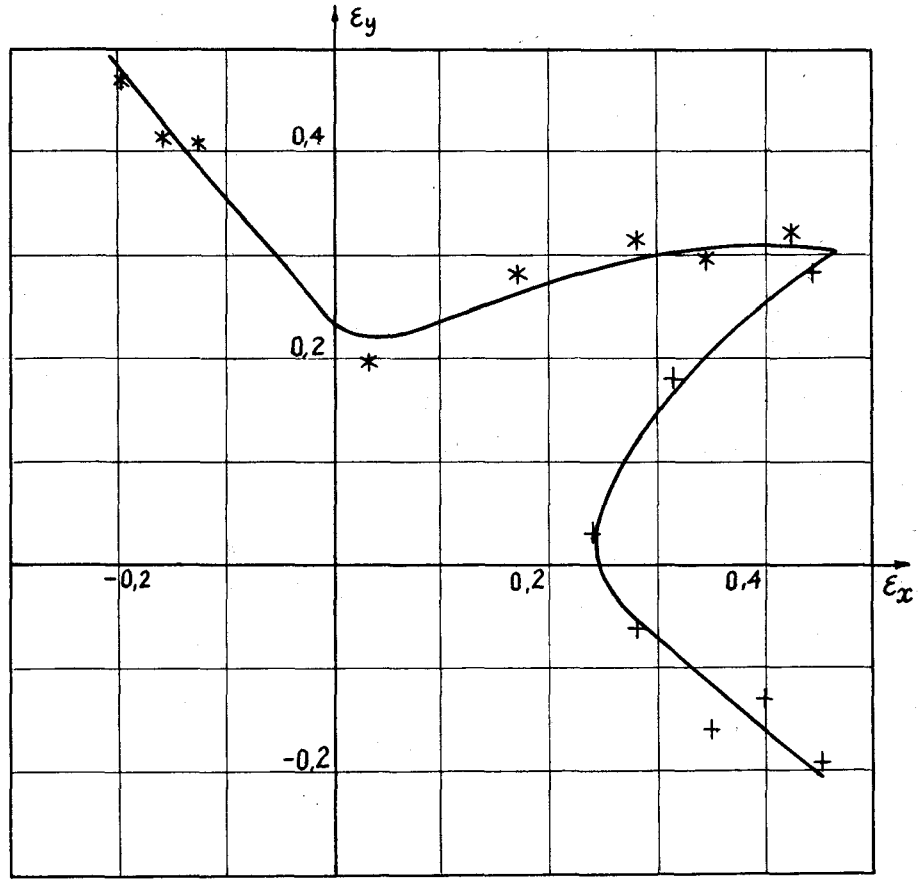

Fig. 2. Forming limit diagrams

* - Rolling direction + - Transverse direction

First and second equations (2.2) can be written in the form

$$\frac{1}{d\lambda}Fd\varepsilon_x = FG(\sigma_x - \sigma_z) + FH(\sigma_x - \sigma_y) \tag{2.5}$$

$$\frac{1}{d\lambda}Gd\varepsilon_y = GF(\sigma_y - \sigma_z) + GH(\sigma_y - \sigma_x). \tag{2.6}$$

From (2.5), (2.6) we have

$$\frac{1}{d\lambda}(Fd\varepsilon_x - Gd\varepsilon_y) = (\sigma_x - \sigma_y)(FG + FH + GH) \tag{2.7}$$

(2.7) can be written

$$\sigma_x - \sigma_y = \frac{1}{d\lambda}\Big(\frac{1}{(FG + FH + GH)}(Fd\varepsilon_x - Gd\varepsilon_y)\Big). \tag{2.8}$$

By analogy, we can obtain

$$\sigma_y - \sigma_z = \frac{1}{d\lambda}\Big(\frac{1}{(FG + FH + GH)}(Gd\varepsilon_y - Hd\varepsilon_z)\Big) \tag{2.9}$$

and

$$\sigma_z - \sigma_x = \frac{1}{d\lambda}\Big(\frac{1}{(FG + FH + GH)}(Hd\varepsilon_y - Fd\varepsilon_z)\Big) \tag{2.10}$$

By substituting (2.8), (2.9), (2.10), (2.4) into (2.3) and rearranging, we can calculate $d\bar{\varepsilon}$ in the form

$$d\bar{\varepsilon}^2 = (G + H)\Big\{\frac{1}{(FG + HF + GH)^2}\big[F(Gd\varepsilon_y - Hd\varepsilon_z)^2 + G(Hd\varepsilon_z - Fd\varepsilon_x)^2$$

$$+ H(Fd\varepsilon_x - Gd\varepsilon_y)^2 + 2\Big(\frac{d\varepsilon_{yz}^2}{L} + \frac{d\varepsilon_{zx}^2}{M} + \frac{d\varepsilon_{xy}^2}{N}\Big)\Big\} \tag{2.11}$$

In the remaining of this paper the following assumptions will be made:

- The sheet is subjected to plane stress and the stress component σ_z normal to the sheet surface is negligible ($\sigma_z \cong 0$).

- σ_x and σ_y coincide with the principal directions of sample. With the above assumptions, (2.3) can be written as follows

$$\bar{\sigma}^2 = \frac{1}{(G + H)}\Big[F\sigma_y^2 + G\sigma_x + H(\sigma_x - \sigma_y)^2\Big]. \tag{2.12}$$

Introducing $d\lambda$ from (2.4) into two first eq. (2.2), we can calculate

$$\sigma_y = \Big[(G + H)d\varepsilon_y - Hd\varepsilon_x\Big] \cdot \frac{\bar{\sigma}}{\Big[(F + \Big(\frac{HG}{(G + H)}\Big)d\bar{\varepsilon}\Big]},$$

$$\sigma_x = \frac{H\sigma_y}{(G + H)} + \frac{\bar{\sigma}d\varepsilon_y}{d\bar{\varepsilon}}. \tag{2.13}$$

From this equations, the forming limit stress curves corresponding to the forming limits strain diagram shown on Fig. 2 have been obtained and presented on Fig. 3.

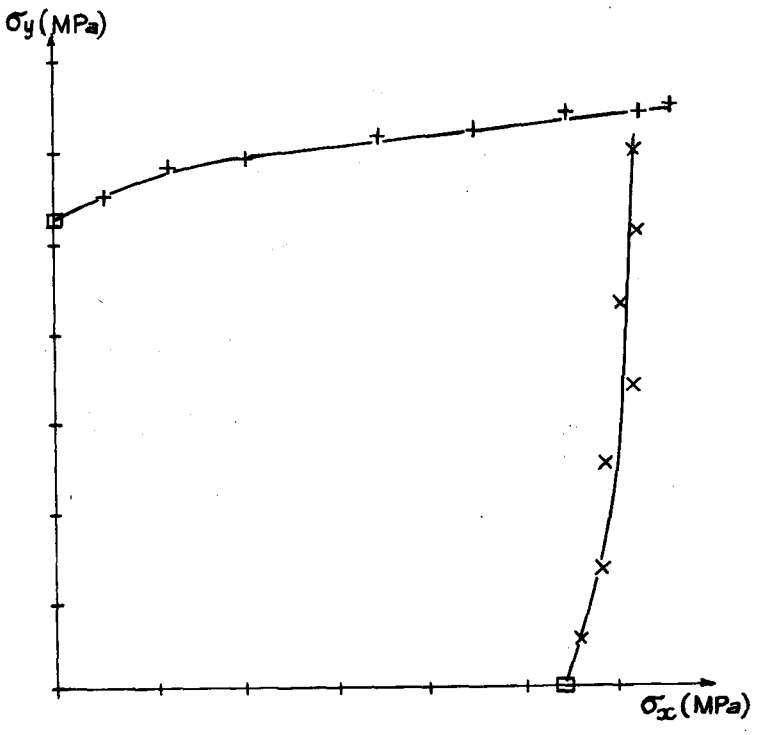

Fig. 3. Forming limits stress curves
+ - Rolling direction, × - Transverse direction

§3. Calculated forming limit strains from the limit stress diagram

For one given stress state defined by σ_x, σ_y on the forming limit stress curve, we can calculate the effective stress by relation (2.12).

The experimental strain hardening curve is obtained $\overline{\sigma} = K\overline{\varepsilon}^n (k = 528,\ n = 0.22)$. It is monotonic, so we can calculate

$$\overline{\varepsilon} = \left(\frac{1}{K}\right)^{1/n} \cdot \overline{\sigma}^{1/n}. \tag{3.1}$$

The strain path is assumed to be composed of two straight segments and the strain state at the end of prestrain is given, so we have

$$\overline{\varepsilon} = d\overline{\varepsilon}_p + d\overline{\varepsilon}_f \tag{3.2}$$

where the index p and f present respectively to the end of prestrain and the end of final strain.

The prestrain state is known $d\varepsilon_x^p$, $d\varepsilon_y^p$, so the effective strain at the end of prestrain can be determined

$$d\bar{\varepsilon}_p^2 = \frac{(G+H)}{(FG+FH+GH)^2}\Big[F(Gd\varepsilon_y^p - Hd\varepsilon_z^p)^2 + G(Hd\varepsilon_z^p - Fd\varepsilon_x^p)^2 + H(Fd\varepsilon_x^p - Gd\varepsilon_y^p)^2\Big]. \tag{3.3}$$

For the second segment the final effective strain can be written

$$d\bar{\varepsilon}_f = \bar{\varepsilon} - d\bar{\varepsilon}_p \tag{3.4}$$

The strains $d\varepsilon_x^f$, $d\varepsilon_y^f$ correspond to final path can be calculated

$$\begin{aligned}(d\varepsilon_y)^f &= \Big[F\sigma_y + H(\sigma_y - \sigma_x)\Big]\frac{d\bar{\varepsilon}_f}{(G+H)}\bar{\sigma},\\ (d\varepsilon_x)^f &= \Big[G\sigma_x + H(\sigma_x - \sigma_y)\Big]\frac{d\bar{\varepsilon}_f}{(G+H)}\bar{\sigma}.\end{aligned} \tag{3.5}$$

So the forming limit strain state is determined.

- So the forming limit strain states are determined for rectilinear or broken strain paths.

- From the forming limit stress curve, we calculate the forming limit diagrams for prestrain by tension and by biaxial stretching.

On the figures 4 and 5 we have drawn respectively the forming limit curves for various levels of prestrain by tension and by equibiaxial stretching.

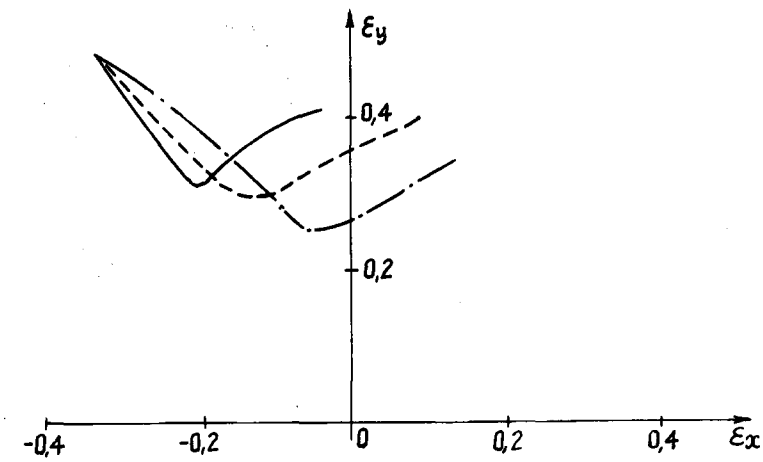

Fig. 4. Forming limit curves for prestrain by tension

—— - Prestrian - 0.1; 0.2, - - - - Prestrain - 0.08; 0.16, —·—. Prestrain - 0.06; 0.12

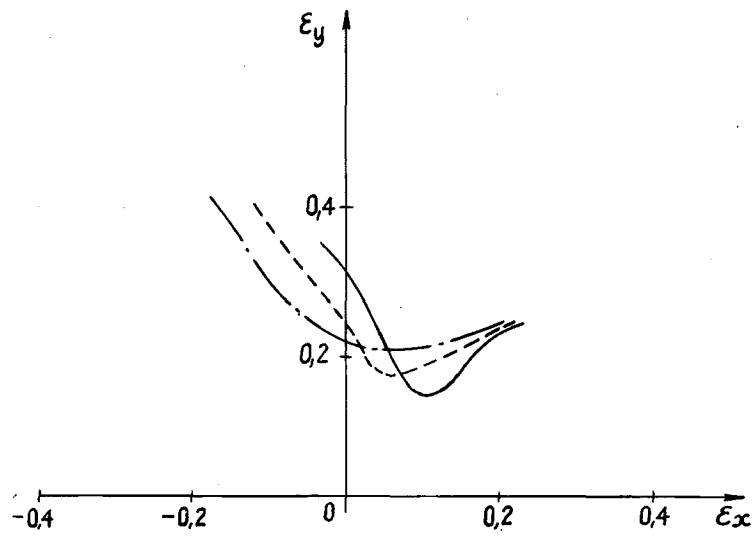

Fig. 5. Forming limit curves for prestrain by stretching
—— - Prestrian - 0.1, - - - - Prestrain - 0.08, —·— . Prestrain - 0.06

We can observe here that for prestrain by tension (Fig. 4), an increasing prestrain value markes the level of the curve higher, while it makes the level of the curve lower for prestrain by biaxial stretching (Fig. 5).

REFERENCES

1. Arrieux R., Bedrin C., Boivin M. Determination of an intrinsic forming limit stress diagram for isotropic sheets, proc. of the 12^{th} IDDRG Congress, Santa Marghrita. Liguire, **2** (1982), 61-71.
2. Arrieux R., Boivin M. Theoretical determination of the forming limit stress curve for isotropic sheet material, CIRP Annals 38/1 (1989), 261-264.
3. Arrieux R., Boivin M. Détermination théorique du diagramme des contraintes limites de formage. Application aux matériaux anisotropes. European Journal Mech. Eng. Vol. 37. No 2 (p.89-96).
4. Bragard A., Baret J. C., Bonnarens H. A simplified method to determine the F. L. D. onset of localised necking. Liège, rapport C.R.M., 1972, n. 33, 35p.
5. Hill R. (eds), Mathematical theory for plasticity, Clarendom Press, Oxford 1950.
6. Nguyen Nhat T., Arrieux R. Off axes forming limit stress diagram of an

anisotropic stell sheet, proc. of the AMPT Conference, Dublin **2** (1993) 1203-1214.

7. Gronostajski L., Dolny K. Determination of the forming limit curve by means of Marciniak's punch, Mem. Sci. rev. Met., **4** (1980), 570-578.
8. Stören S., Rice J. R. Localized necking in thin sheets, J. Mech. Phys. Solids, **23** (1975), 421-441.
9. Danckert J. Determination of instability in sheet metal based on the anisotropic yield ellipse. Annals of the CIRP, Vol 40/1/1991.
10. Mariciniak Z. and Kuczynski K. Limit strains in the processes of stretch-forming sheet metal. Int. J. Mech. Sci. Pergamon Press Ltd. **9** (1967), 609-620.
11. Nguyễn Nhật Thăng. Détermination de l'influence du trajet de déformation sur la courbe limite de formage, Journal of Mechanics, NCNST of Vietnam T.XVIII, No.3, 1996, 33-39.

Received November 25, 1998

NGHIÊN CỨU ẢNH HƯỞNG CỦA BIẾN DẠNG CHO TRƯỚC CHO VIỆC DỰ ĐOÁN SỰ CỐ XẢY RA CO THẮT

Các kết quả thực nghiệm xác định các đặc trưng cơ học của tấm thép ít các bon được giới thiệu ở đây.

Nghiên cứu ảnh hưởng của biến dạng trước từ đường cong ứng suất giới hạn được xác định theo hướng cán và hướng ngang của tấm tôn thép.

Hanoi University of Technology
1 Dai Co Viet Str., Hanoi, Vietnam